Light Scattering and Cryo-Transmission Electron Microscopy Investigation of the Self-Assembling Behavior of Di-C_{12}P-Nucleosides in Solution

Francesca Baldelli Bombelli,[†] Debora Berti,*[,†] Mats Almgren,[‡] Göran Karlsson,[‡] and Piero Baglioni*[,†]

Department of Chemistry and CSGI, University of Florence, Florence, Italy, and Department of Physical and Analytical Chemistry, Uppsala University, Box 579, SE-75123 Uppsala, Sweden

Received: January 27, 2006; In Final Form: May 17, 2006

Aggregates formed from freshly prepared and annealed samples of dilauroyl-phosphatidyl-adenosine, dilauroyl-phosphatidyl-uridine, and their 1:1 mixture have been investigated by dynamic light scattering, cryo-transmission electron microscopy (cryo-TEM) observations, and circular dichroism. The two surfactants differ only for the nucleoside at the phospholipid polar headgroup and self-assemble in solution to form supramolecular structures that behave dissimilarly. The uridine derivative forms long wormlike aggregates that are invariant with the aging of the solution, while the wormlike aggregate of the adenosine derivative undergoes, as the sample ages, a subsequent self-assembling process forming giant helicoidal aggregates that coexist with the smaller wormlike aggregates. Dynamic light scattering and cryo-TEM show that the large helicoidal structures are formed at the expense of the small wormlike micelles. The 1:1 mixture behaves as the adenosine derivative and evolves to form giant superstructures for all the lipid concentrations investigated. Circular dichroism measurements suggest that the formation of the supramolecular helicoidal structure might not be driven by a purely chiral effect, but rather stacking and hydrogen bonding, present at the phospholipid headgroups of the self-assembled nucleosides, contribute to the final supramolecular structure.

Introduction

One of the most important classes of biopolymers, DNA and RNA, represent an unrivalled example where supramolecular chemistry is used to store, transmit, and replicate information in water (a challenging environment for base−base hydrogen bond formation) with a limited number of structural units (adenine, cytosine, guanine, thymine, and uracil).

Molecular recognition triggered by self-assembly of various surfactants with nucleic acid base polar heads was prompted some years ago by a study of self-organization of some nucleic-acid-functionalized amphiphiles arranged at the air/water interface and has since then continued to attract considerable and ever growing attention.[1]

In this research field, we focused our attention on a class of compounds having close chemical relationships with nucleic acid monomers. These compounds, called phosphatidylnucleosides (PLNs), are composed of a phospholipid backbone and a nucleotide polar head that reproduce the chemistry and the charge of each DNA monomer, hold biological relevance, and are also promising in medical and pharmaceutical applications and possibly for nonviral gene therapy.[2−5]

Self-assemblies of these biosurfactants are characterized by the dynamic noncovalent nature of auto-organization forces; the responsiveness to soft external stimuli is integrated and enriched by the presence of additional energetic contributions due to the presence of "smart" nucleic acid polar heads.

The interfacial curvature of self-assemblies is mainly dictated by the choice of the hydrophobic assembler, i.e., the phospholipid backbone. Globular, rigid, or flexible cylindrical micelles or bilayers can be formed as a result of packing preferences of the constituting surfactant molecule. However, in PLN the nature of the polar head provides a molecular specificity that fine-tunes aggregation, and the geometry of spontaneous self-assembly and the interfacial film properties are the result of a delicate balance between hydrophobic forces and polar head interactions. Base−base interactions are, therefore, triggered by aggregation and are themselves responsible for structural modulations of the assembly.

We have studied base−base interactions in bilayered closed vesicles[6−8] and in micellar aggregates,[9,10] notwithstanding the exposure of the bases to an aqueous environment that is a formidable competitor for hydrogen bonding and the formation of base−base hydrogen bonding.

More recently our attention has been drawn to the study of semiflexible wormlike aggregates, also called polymer-like micelles, or living polymers, formed by dilauroylphospholipo-nucleosides (DLPNs).[11] We have focused our studies on two representative derivatives of the dilauroyl group, namely, adenosine (DLPA) and uridine (DLPU). These bases have very different π-stacking attitudes, since uridine is a poor homo-stacker, while adenosine, like all purines, has a higher stacking tendency. On a macromolecular length scale this is transferred to the different solution structures of poly-adenosine and poly-uridine. Moreover, adenosine and uridine are RNA complementary bases, so that the A−U hydrogen-bond adduct is preferred over the three possible combinations.

DLPU has been characterized in aqueous solution through a combination of small-angle neutron scattering and static light scattering and over a wide concentration and salinity range. These studies have highlighted micellar growth with increasing lipid concentration and salinity to giant flexible wormlike

* Authors to whom correspondence should be addressed. Phone: +39 055-457-3038 (D.B.); +39 055-457-3033 (P.B.) Fax: +39 055-457-3032 (P.B.). E-mail: berti@csgi.unifi.it.; baglioni@csgi.unifi.it.

[†] University of Florence.

[‡] Uppsala University.

10.1021/jp060594d CCC: $33.50
Published on Web 08/17/2006

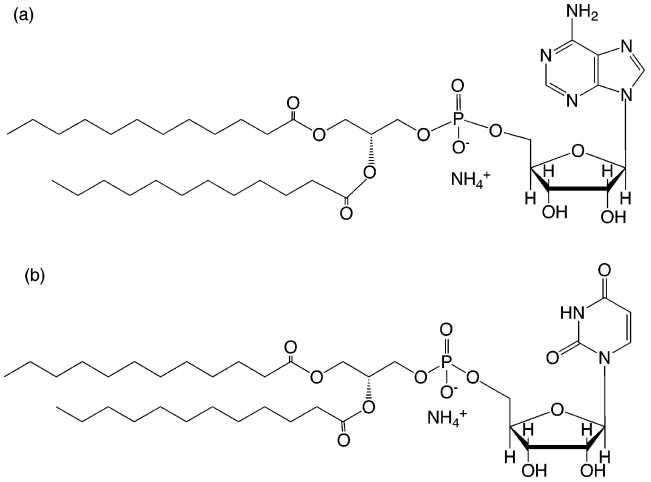

Figure 1. Schematic drawings of the chemical structures of (a) dilauroyl-phosphatidyl-adenosine and (b) dilauroyl-phosphatidyl-uridine.

aggregates that eventually entangle to form a transient network with response to mechanical stress similar to polymer solutions in the semidilute range.[12,13]

The chemistry of biologically relevant polar heads can imply mutual interactions in the aggregate not limited to electrostatic repulsions or to excluded volume.

To explore this possibility, we have undertaken a structural study on the aggregates formed by the analogous adenosine derivative that is the subject of this paper. Moreover, to highlight Watson−Crick-like specificity, the properties of a 1:1 mixed system (DLPM) have been compared with binary micellar phases.

Dynamic light scattering provides evidence of structural information on the mesoscale that can be usefully supported by cryo-transmission electron microscopy (cryo-TEM) obervations. A correlation with base electronic properties is then obtained through circular dichroism (CD).

Materials

1,2-Dilauroyl-*sn*-glycero-3-phosphocholine (DLPC) was purchased from Avanti Polar Lipids (Alabaster, AL), and its purity was checked by thin-layer chromatography. The lecithin was used as received since no oxidation or lyso products were not detected. Uridine, HCl, $CHCl_3$, MeOH, and NH_3 (33% aqueous solution) used in the synthesis and NaH_2PO_4(≫99%) and Na_2HPO_4 (≫99%) were purchased from Fluka (Switzerland). Phospholipase D from *Streptomyces* sp. AA586 was a generous gift from Asahi Chemical Industry Co., Ltd. (Tokyo, Japan).

Synthesis of Dilauroyl-Phosphatidyl-Nucleoside. DLPU and DLPA were synthesized starting from the corresponding phosphatidylcholine in a two-phase system according to a modification of the method proposed by Shuto and co-workers[14] and obtained as an ammonium salt. A chloroform solution of the nucleolipid was added to an acetate buffer solution containing the nucleoside and the phospholipase D. The mixture was stirred vigorously at 45 °C for at least 3 h. HCl (2 N), MeOH, and $CHCl_3$ were added, and then the organic layer was washed with water and dried. The product was purified by stepwise elution flash chromatography, and the acidic form of the phosphatidylnucleoside was converted into the ammonium salt to avoid product degradation. The molecular structures of the two nucleolipids are reported in Figure 1.

Sample Preparation. DLPN samples have been prepared by adding the lyophilized powder to the buffer solution and have been measured as soon as they have been completely dissolved. We also have investigated annealed samples stored in a controlled water bath at 25 °C after 1, 2, and 4 days.

Methods

Dynamic Light Scattering. Light scattering measurements were performed on a Brookhaven Instrument apparatus equipped with a BI9000AT correlator and a BI200SM goniometer. The signal was detected by an EMI 9863B/350 photomultiplier. The light source was the second harmonic of a diode-pumped Coherent Innova Nd:YAG laser ($\lambda = 532$ nm), linearly polarized in the vertical direction. Measurements were performed at 25 °C. Approximately 1 mL of sample solution was transferred into the cylindrical Hellma scattering cell that was then sealed and centrifuged for about 1 h at 5000*g* to remove dust particles from the scattering volume.

In dynamic light scattering (DLS) experiments, the normalized time autocorrelation function $g_2(q,t)$ of the scattered intensity is measured according to

$$g_2(q,t) = \frac{\langle I^*(q,0)I(q,t)\rangle}{\langle I(q,0)^2\rangle} \tag{1}$$

For ergodic systems, this function can be expressed in terms of the field autocorrelation function $g_1(q,t)$ through the Siegert relation

$$g_2(q,t) = A[1 + \beta^2 g_1(q,t)^2] \tag{2}$$

where A is the baseline and β^2 is the coherence factor dependent on the scattering geometry and details of the detection system. When the spectral profile of the scattered light can be described by a multi-Lorentzian curve, $g_1(q,t)$ can be written as the Laplace transform of the spectrum of relaxation times

$$g_1(q,t) = \int_0^\infty w(\tau)\, e^{-t/\tau}\, d\tau \tag{3}$$

where τ is the relaxation time characteristic of the system and $w(\tau)$ is its weight factor in the relaxation time distribution.

To obtain a distribution $w(\tau)$ of decay rates, a constrained regularization method, CONTIN, developed by Provencher,[15] was used to invert the experimental data. A statistical parameter "probability to reject", P, is calculated for each $w(\tau)$ generated by CONTIN. The preferred solution is usually the one characterized by a P value closest to 0.5.

Cryo-TEM. The preparation of the samples for cryo-TEM investigation has been performed[16] as follows: A small droplet of the solution was placed under controlled conditions on a pretreated Cu grid of about 20 μm in thickness, which was covered by a perforated cellulose acetate butyrate film. Excess material was removed by a gentle wiping with a filter paper. The specimen was vitrified by a rapid transfer into liquid ethane close to its freezing temperature. The sample examination was performed with a Zeiss 902A electron microscope operating at 80 kV and 100 K. The temperature of the specimen was kept below −165 °C during both transfer to the microscope and examination. Images were recorded under focus settings of about 2−3 μm to enhance the image contrast.

Circular Dichroism. Circular dichroism spectra have been collected on a J-715 Jasco spectro-polarimeter. Hellma quartz cylindrical cells with variable path lengths were selected so that samples do not exceed 0.8 optical density. The observed circular dichroism was converted into molar ellipticity, normalizing for path length and dichroic chromophore concentration.

Results and Discussion

DLPA and DLPU Self-Assembling Behavior. To detect how the different base nature affects the aggregation process,

dilauroylphosphonucleosides have been studied through DLS as a function of time in 0.1 M phosphate-buffered saline (PBS) solutions at pH = 7.5.

Previous scattering results[12,13,17] on DLPU, which differs from DLPA in the base at the polar head (uridine is the pyrimidine complementary to adenosine in RNA), support the formation of flexible cylindrical micelles already at low surfactant volume fractions ($\phi = 0.06\%$). The phase behavior of DLPU micellar solutions as a function of surfactant concentration and medium salinity, M, shows[12] the growth of the average contour length with increasing lipid volume fraction. Above the so-called "crossover concentration" these flexible aggregates begin to overlap to form a micellar network. This microscopic structural change is macroscopically highlighted by the appearance of viscoelastic properties.

In this paper, the phase behavior of 4 mM nucleolipid micellar solutions of DLPA and DLPU has been obtained through DLS measurements of freshly prepared and annealed solutions. At this concentration, surfactants are in the dilute regime, and the uridine derivative autocorrelation function is monomodal, making the detection of possible changes in the autocorrelation functions due to the formation of different aggregates for the adenine derivative easy.

The dynamic properties of DLPU are invariant with the aging of the solution while the autocorrelation functions of DLPA show the appearance of a slower relaxation for the annealed sample. A detailed DLS analysis for the DLPU system already has been reported. [12]

Figures 2A−C report the DLPA autocorrelation functions at different scattering angles for freshly prepared, 1 day annealed, and 4 day annealed at 25 C micellar solutions; after this period no changes in the micelles' dynamic properties have been observed.

The intensities of the autocorrelation functions of the freshly dissolved sample are dominated by a single relaxation time, as expected in this concentration regime; a second slower relaxation time becomes more and more evident as a function of the annealing time. A log−log representation of the autocorrelation functions at the same scattering angle (Figure 3A) highlights the presence of two well-separated populations for annealed samples. A Laplace inversion of these autocorrelation functions, performed with the algorithm CONTIN, gives the relaxation time distributions shown in Figure 3B.

The CONTIN analysis of the autocorrelation functions yields the mean relaxation rate Γ (s^{-1}) for both the fast and the slow modes. Autocorrelation functions that describe spatial concentration fluctuations decay through a diffusive mechanism, and $[g_2(q,\tau) - 1]$ has the following exponential form

$$[g_2(q,\tau) - 1] \propto \exp(-\Gamma t) \qquad (4)$$

where $\Gamma = D_c{*}q^2$ and D_c is the collective diffusion coefficient. Figure 4A shows the linear dependence of this fast relaxation decay on the squared scattering vectors for the same sample at different annealing times, and Table 1 collects the resulting diffusion coefficients. The diffusion coefficient associated with the fast mode decreases with annealing, suggesting that even the smaller assembled structures undergo a micellar growth. A further issue that supports the attribution of this fast mode to the diffusion of relatively smaller threadlike objects is obtained from the comparison with DLPU collective diffusion coefficient, at the same surfactant volume fraction, that is of the same order of magnitude (4.7×10^{-8} cm^2 s^{-1}),[12]

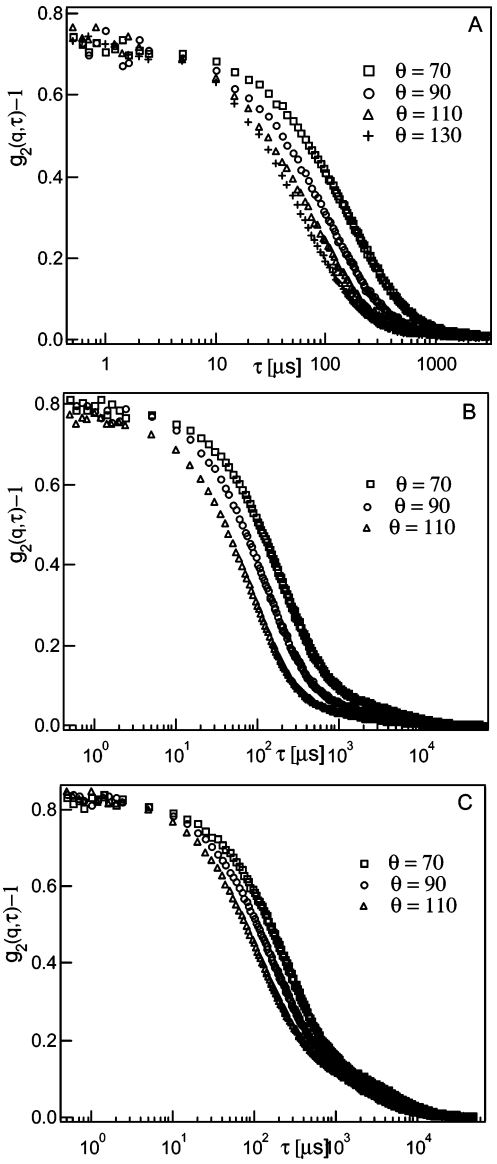

Figure 2. DLS autocorrelation functions for 4 mM DLPA micellar solutions in 0.1 M PBS at pH = 7.5 at different scattering angles θ: (A) sample just prepared; (B) sample annealed for one day at 25 °C; (C) sample annealed for 4 days at 25 °C.

ascribed to a "pure" diffusive mode of the micellar wormlike phase.

A linear q^2 dependence has been found for the slower mode as well, as reported in Figure 4B, indicating again the diffusive nature of this population. The resulting diffusion coefficient is invariant for 1 and 4 day annealed samples but becomes prevalent with sample aging, as suggested by both the autocorrelation functions and CONTIN relaxation time distributions (Figure 3).

In conclusion, the DLS investigation of DLPA shows the formation of a wormlike phase that undergoes, as the sample ages, a self-assembling process to form larger giant aggregates coexisting with the smaller ones, whose diffusion is responsible for the slow decay of concentration fluctuations.

Cryo-TEM Analysis. Further information about the morphology and the shape of the larger structures has been obtained through a cryo-TEM investigation on DLPU and DLPA micellar solutions in the dilute regime, as a function of surfactant concentration and aging time.

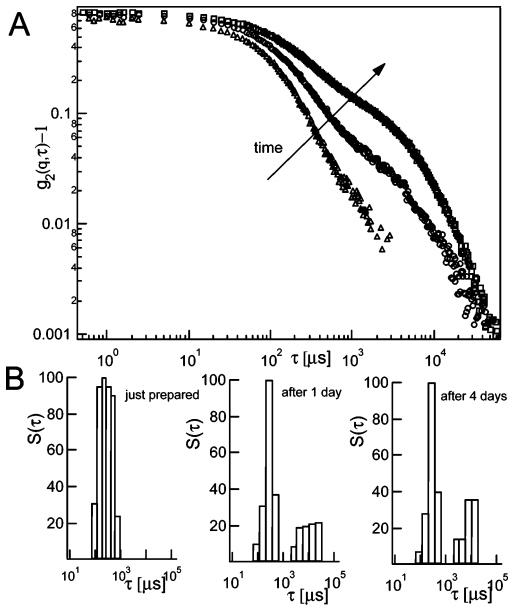

Figure 3. (A) The log−log representation of DLS autocorrelation functions for 4 mM DLPA micellar solutions at a scattering angle $\theta = 90°$: (△) just prepared; (○) annealed for 1 day; (□) annealed for 4 days. (B) CONTIN analysis of autocorrelation functions reported in part A. For annealed samples, we determine two separated populations.

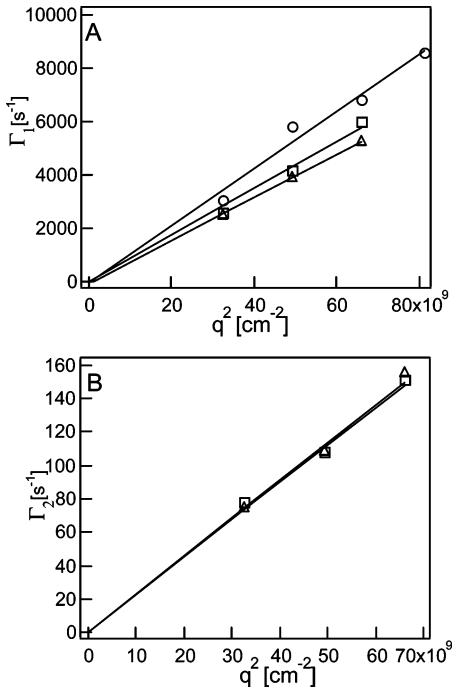

Figure 4. Relaxation modes of 4 mM DLPA solution as a function of the scattering angle squared. (A) Behavior of Γ_1 (s^{-1}) (fast mode) vs q^2 (cm^{-2}): (○) freshly prepared; (□) annealed for 1 day; (△) annealed for 4 days. (B) Behavior of Γ_2 (s^{-1}) (slow mode) vs q^2 (cm^{-2}): (□) annealed for 1 day; (△) annealed for 4 days. The collective diffusion coefficients D_c (cm^{-2} s^{-1}) are obtained from the slopes of these fitting curves.

Figures 5A and 5B report the images of 4 and 10 mM DLPU solutions ($\phi = 0.23\%$ and 0.6%, respectively): The pictures show the presence of long wormlike aggregates, confirming the scattering results.

Cryo-TEM investigations on DLPU samples annealed at 25 °C for 96 h have not revealed any changes in self-assembled structures that appear stable.

TABLE 1: Experimental Diffusion Coefficients for a 4 mM DLPA Micellar Solution Obtained from DLS Measurements

time	D_c fast (cm^2/s)	D_c slow (cm^2/s)
freshly prepared	$1.1 \times 10^{-7} \pm 3\%$	
after 1 day	$8.7 \times 10^{-8} \pm 6\%$	$2.3 \times 10^{-9} \pm 6\%$
after 4 days	$7.9 \times 10^{-8} \pm 2\%$	$2.3 \times 10^{-9} \pm 3\%$

As expected, the adenosine surfactant shows a more complex phase diagram exhibiting a time-dependent self-assembling behavior for each lipid concentration investigated. Figures 6A−F report some representative cryo-TEM micrographs of DLPA micellar solutions, as a function of surfactant concentration, just after lipid dissolution (left side) and annealed for 2 days at 25 °C (right side). Freshly prepared solutions (Figures 6A, 6C, and 6E) are mostly composed of threadlike micelles whose cross section size, about 5−6 nm, is invariant with surfactant concentration while the axial dimension grows with increasing lipid volume fraction. However, in more concentrated samples, longer and thicker filaments (cross section size about 7 nm) whose local structure always seems cylindrical are present. From the observation of images at larger magnification (Figure 7A), we can speculate that these giant elongated aggregates derive from the association of smaller micelles that, at this enlargement, appear in some cases as helical filaments.

We observed for annealed DLPA micelles an evolution to long twisted objects. To understand the formation of twisted

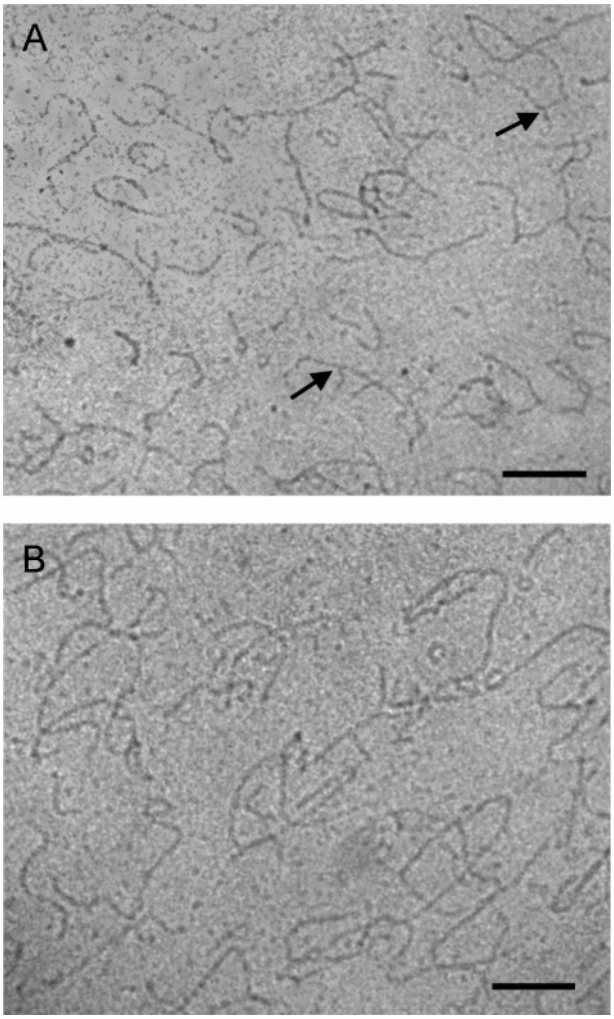

Figure 5. Cryo-TEM micrographs of DLPU micellar solutions in 0.1 M PBS pH = 7.5: (A) 4 mM; (B) 10 mM. Both images show wormlike micelles polydisperse in their contour lengths. The arrows indicate a 3-fold junction. The scale bar is 100 nm.

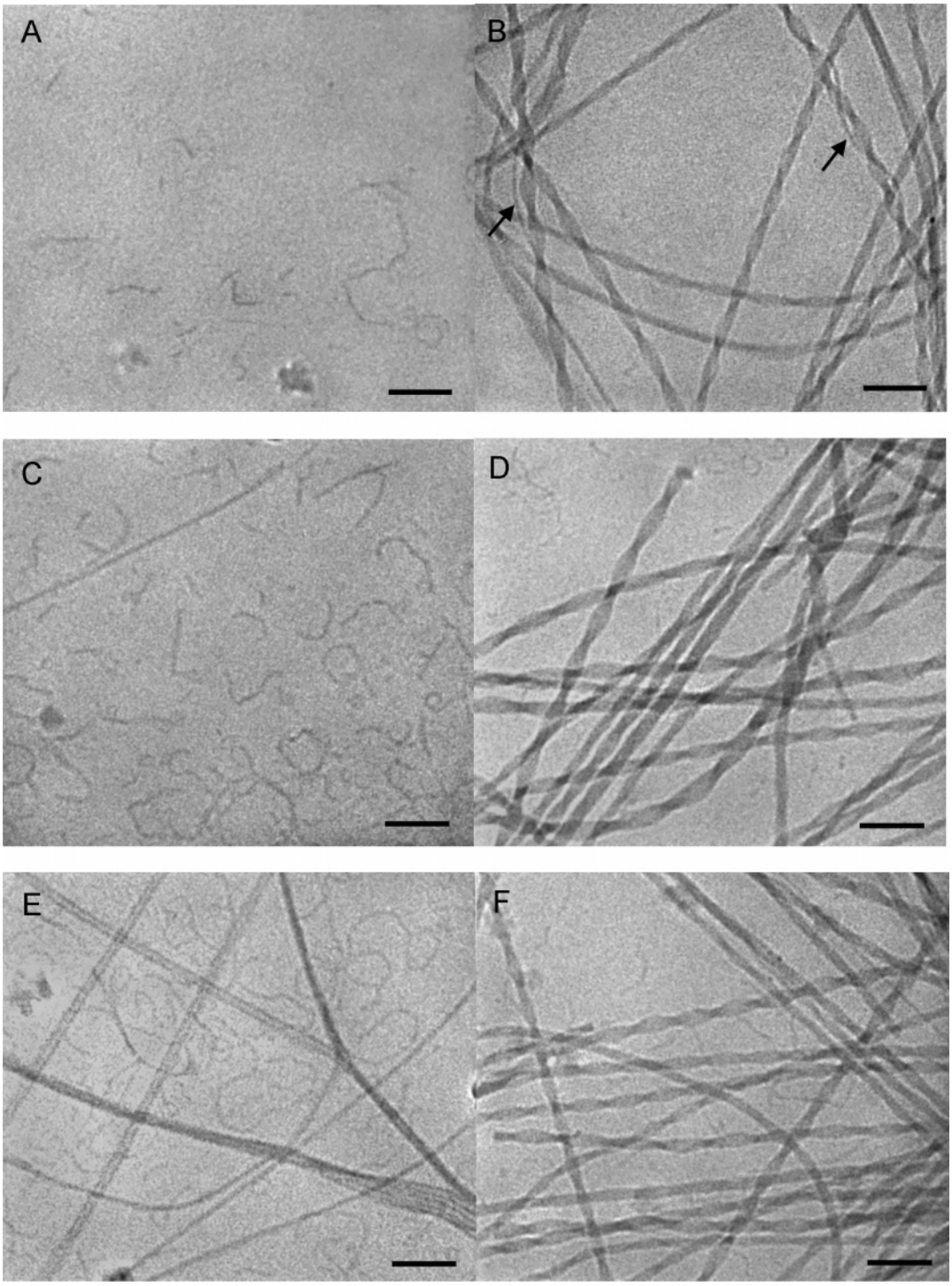

Figure 6. Cryo-TEM images of DLPA micellar solutions in 0.1 M PBS pH = 7.5. On the left samples just after the preparation at 25 °C are shown; on the right the same samples annealed at 25 °C for 2 days are shown. The arrows indicate the twisting of a single cylindrical micelle around to a helical superstructure. DLPA concentrations: (A and B) 1 mM; (C and D) 4 mM; (E and F) 10 mM. The scale bar is 100 nm

objects, particularly explicative is Figure 7B where twisting seems to be favored when several single filaments are joined together. This process can be also observed in Figure 6E where some parallel giant threads begin to kink together and in Figure 6B where the arrow indicates a peculiar image of a single thick helical filament helically wound around a just formed twisted aggregate.

The phase evolution to form helical suprastructures occurs at the expense of smaller threadlike micelles, whose global content averagely increases with surfactant concentration in both fresh and annealed samples. The thickness and the helical pitch of these objects are not constant, but their ratio is almost invariant (considering the largest thickness the ratio is around 0.3); hence they probably change according to the number of threads of which they are composed as simple geometrical rules suggest.

Similar self-assembled helical structures in aqueous solutions have been observed for amphiphilic peptides,[18,19] for diacetilenic lipids,[20] for long-chain nucleolipids, [21] and for gemini surfactant in the presence of chiral counterions.[22] Several models have been developed to explain the formation of this kind of aggregates, and a recent review paper [23] groups these models

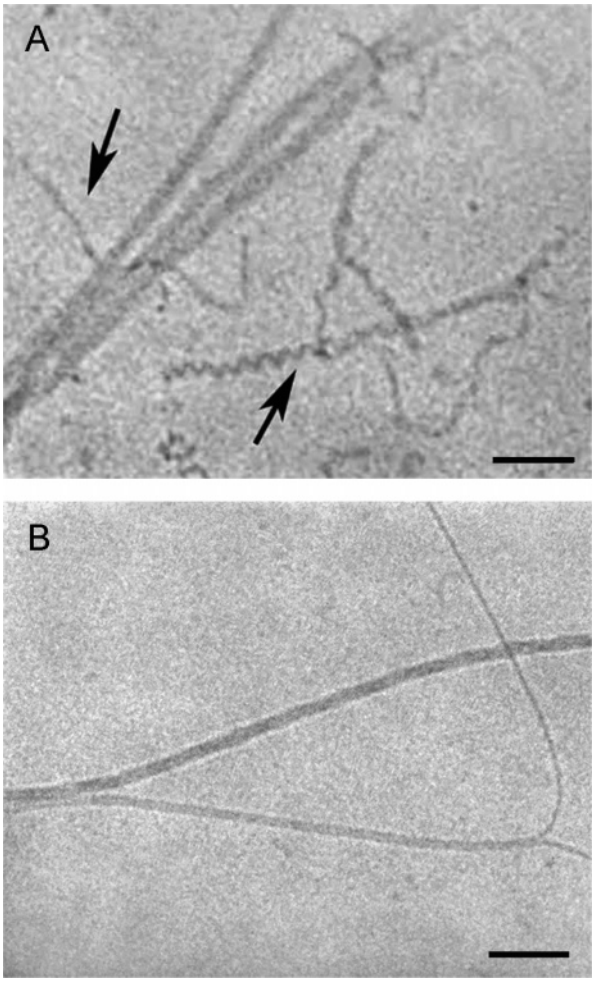

Figure 7. (A) Magnification of smaller micelles present in DLPA solutions demonstrating the helical shape and "micelle" tendency to twist. (B) Example of larger self-assembled structures present in DLPA micellar solutions. The scale bar is 100 nm.

in two categories: models based on chiral elastic properties of the membranes and models based on other effects, including electrostatic interactions, elasticity, and spontaneous curvature.

It is well-known that the spontaneous curvature of the surfactant film, determined by the surfactant chemical nature and by the dispersing medium, induces different self-assembled morphologies and that the molecular shape of the surfactant (i.e., packing parameter) sets the tilt between neighboring molecules in the aggregate. Chiral surfactants, once self-associated, could require optimization of the head−head interaction, a preferred orientation that imposes a twist of the aggregate interface. Actually, the relation between twist and chirality remains debated, and an experimental control over the expression of the chirality of the constituent molecules in self-assembled structures is hardly achievable since other effects, such as specific interactions between polar heads and/or packing constraints, come into play.The combination of all these effects makes the attainment of fine-tuned supramolecular chiral structures difficult on a molecular scale. [24]

In our case, the resolution of the images does not always allow the determination of the helical handedness, but a careful check of all the micrographs has highlighted the presence of right- and left-handed twisted aggregates, unluckily without any apparent trend. This experimental evidence suggests that the formation of helical aggregates is not driven by a purely chiral effect.

However, the two nucleolipids are characterized by the same alkyl chain, and they *only* differ in nucleic base nature; their molecular features are not so much different ($V_{DLPU} \approx$ 1050 Å^3 and $V_{DLPA} \approx$ 1080 Å^3), and their steric hindrances are very similar: We cannot therefore ascribe the more complex aggregational behavior of DLPA to simple different packing constraints.

The self-aggregation mechanism is mainly driven by the hydrophobic effect that is principally due to an entropic gain deriving from the exclusion of hydrocarbon chains from water contact and is identical for the two derivatives; hence the different self-association behavior of DLPA versus DLPU can be explained considering an additional contribution, i.e., an enthalpic contribution associated with the base−base interaction at the micelle surface. We already demonstrated that both stacking and hydrogen bonding are active in self-assembling of phospholiponucleosides[1,6,9−11] and the different capacities of uridine and adenosine to establish these interactions can justify the different aggregation behaviors. Comparing the NMR chemical shift (data not reported) of the DLP derivatives to those of the corresponding monomer monophosphate and of the corresponding dioctylphospholiponucleoside spherical micelles we found a significant upfield shift of the proton resonances of the base. This shift is larger for adenine protons. We have also observed a downfield shift of the NH_2 protons indicating the formation of hydrogen bonds upon micellization that is of the same magnitude as that found for spherical aggregates (C8 derivative). The latter two observations point out that the helicoidal supramolecular organization seems to be promoted by base−base stacking interactions.

Moreover, thermodynamic parameters for purine and pyrimidine nucleosides in aqueous solution indicate that (1) the association stacking constants, K, are characteristic of weak interactions and (2) both the enthalpies, ΔH, and the entropies, ΔS, are negative (enthalpic gain). The Gibbs free energy for the dimerization via stacking of nucleosides in aqueous solutions gives rise to negative values for adenosine (−1 kcal/mol) and slightly positive values for uridine (0.29 kcal/mol), both of the same order of magnitude as the thermal energy k_BT. In oligo and polynucleotides, where bases are linked to each other, stacking interactions between adjacent bases occur and give rise to stable, single-stranded helical structures; the stability of these helices reflects the same trend as given above, with poly(A) mainly helical and poly(U) predominantly random coil at room temperature.[25] Furthermore, NMR experiments show that stacking interactions between purine and pyrimidine bases follow the trend: purine−purine > purine−pyrimidine > pyrimidine−pyrimidine. [26,27]

A reasonable working hypothesis for the differences found for the DLPA and DLPU systems is that an additional contribution to the aggregation can derive from stronger adenosine−adenosine stacking interactions at the DLPA polar heads with respect to those present at the surface of the DLPU aggregates. In this case, an intramolecular and intermolecular coordination through stacking and hydrogen-bonding interactions could favor the formation of twisted structures where a saddlelike curvature, better than a cylindrical or flat one, can tune the distance between interacting bases. The resulting self-assembled structure is determined by the subtle balance between the base−base interaction and the surfactant packing preferences. Furthermore, the presence of helical superstructures, characterized by different pitches and thicknesses, could be due to a too densely populated polar headgroup surface so that the preferred interaction distance among the bases does not always respect the packing constraints

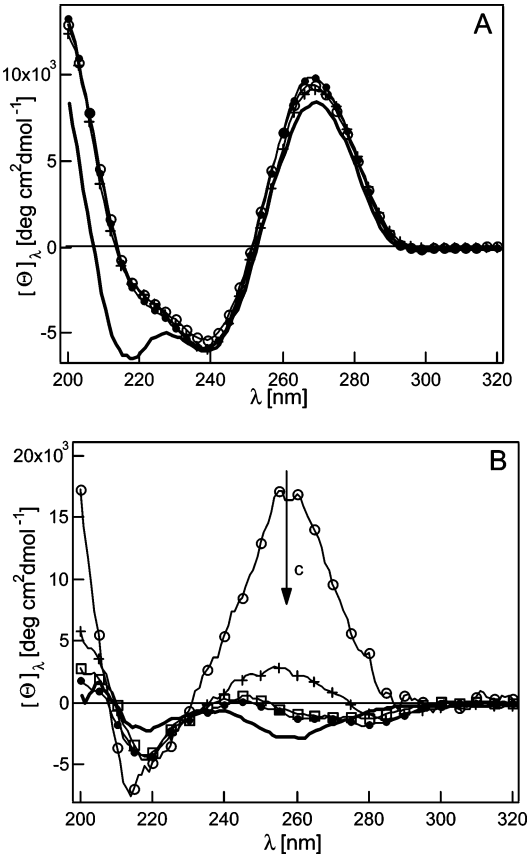

Figure 8. Concentration dependence of CD spectra for (A) DLPU and (B) DLPA micellar solutions in 0.1 M PBS pH = 7.5. Corresponding nucleosidic monophosphate monomer spectra (solid line), UMP and AMP (10 mM), are reported in the same medium as well. The arrow indicates increasing DLPA concentrations. Surfactant concentrations: (○) 1 mM; (+) 4mM; (●) 10 mM; (□) 20 mM.

required by the chemical structure of the lipid. This last point is supported by preliminary results (not reported) obtained diluting the nucleolipid density at the surface of the aggregate by adding a surfactant with the same chain length (sodium dodecyl sulfate (SDS)). The mixed system showed for some SDS/DLPA ratios helical aggregates characterized by the same structural parameters (pitches and thicknesses).

In conclusion, cryo-TEM results confirm DLS findings and point out the continuous evolution of the system to form large structures. The decrease of the fast diffusion coefficient as a function of the annealing time is evidence that superstructures are formed from the aggregation of smaller micelles. Moreover, the different morphologies of DLPA and DLPU self-assembled superstructures are strictly correlated to the different stacking and hydrogen-bonding attitude interactions between the bases at the interface of the nucleolipid "micelle".

Circular Dichroism Experiments: Dependence on Nucleolipid Concentration and Micellar Annealing. Circular dichroism experiments, performed on DLPA and DLPU micellar solutions, provide insights on base−base interactions at the interface, allowing a correlation between structural features of the aggregates and electronic properties of the nucleic bases at the interface.

Information on the electronic structure of nucleic bases has been extensively reported in classic nucleic acid literature. Chromophores themselves have a plane of symmetry and do not show intrinsic CD.[26−29] However, nucleosides and nucleotides do show a low-intensity CD induced by interactions of the base with the asymmetric sugar. Macromolecular structuring

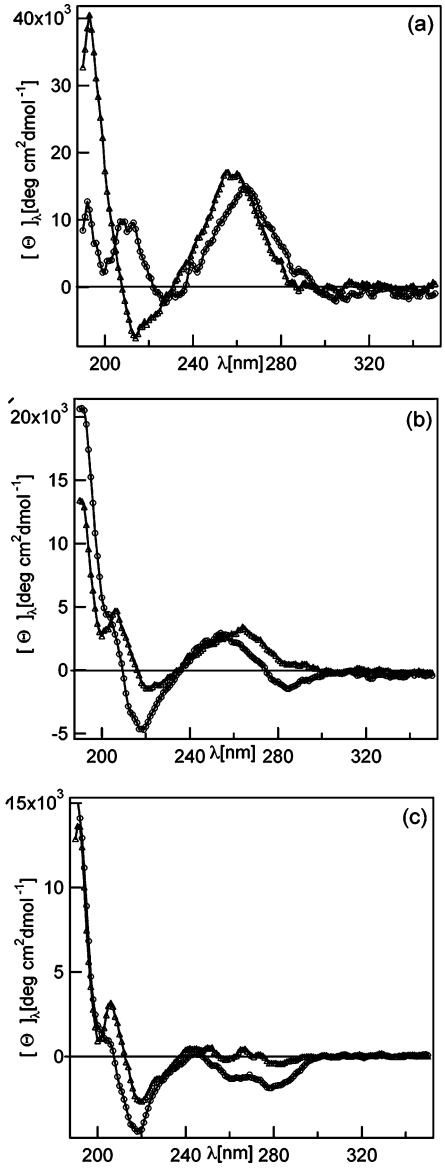

Figure 9. CD spectra of DLPA micellar solutions in 0.1 M PBS at pH = 7.5 as a function of the time: (○) after 1 day; (△) after 3 days. (a) DLPA 1×10^{-3} M; (b) DLPA 4×10^{-3} M; (c) DLPA 1×10^{-2} M.

in nucleic acid and in polynucleotides (e.g., helical conformation) due to base−base interactions such as stacking, can further induce a so-called *super-asymmetry* that enhances the dichroism of UV absorption bands. CD is therefore an extremely sensitive method for monitoring both the conformation of nucleic acids and polynucleotides and their response to external stresses.

We have first investigated DLPU and DLPA micellar solutions as a function of surfactant concentration; Figures 8A and 8B show DLPU and DLPA spectra in the lipid concentration range 1−20 mM. The figures also show the CD spectra of the corresponding monophosphate monomers (dotted line); the choice to refer CD spectra of the micellized surfactant to the mononucleotide ones is to extract information about the possible excess of base−base interactions induced by the arrangement in a supramolecular aggregate.

CD spectra of DLPU do not show dependence on surfactant concentration and are almost identical to the those of UMP, except for a slight difference at lower wavelengths in the negative band, due to the different substitution of the phosphate in the case of the surfactant. Hence, CD indicates a similar base

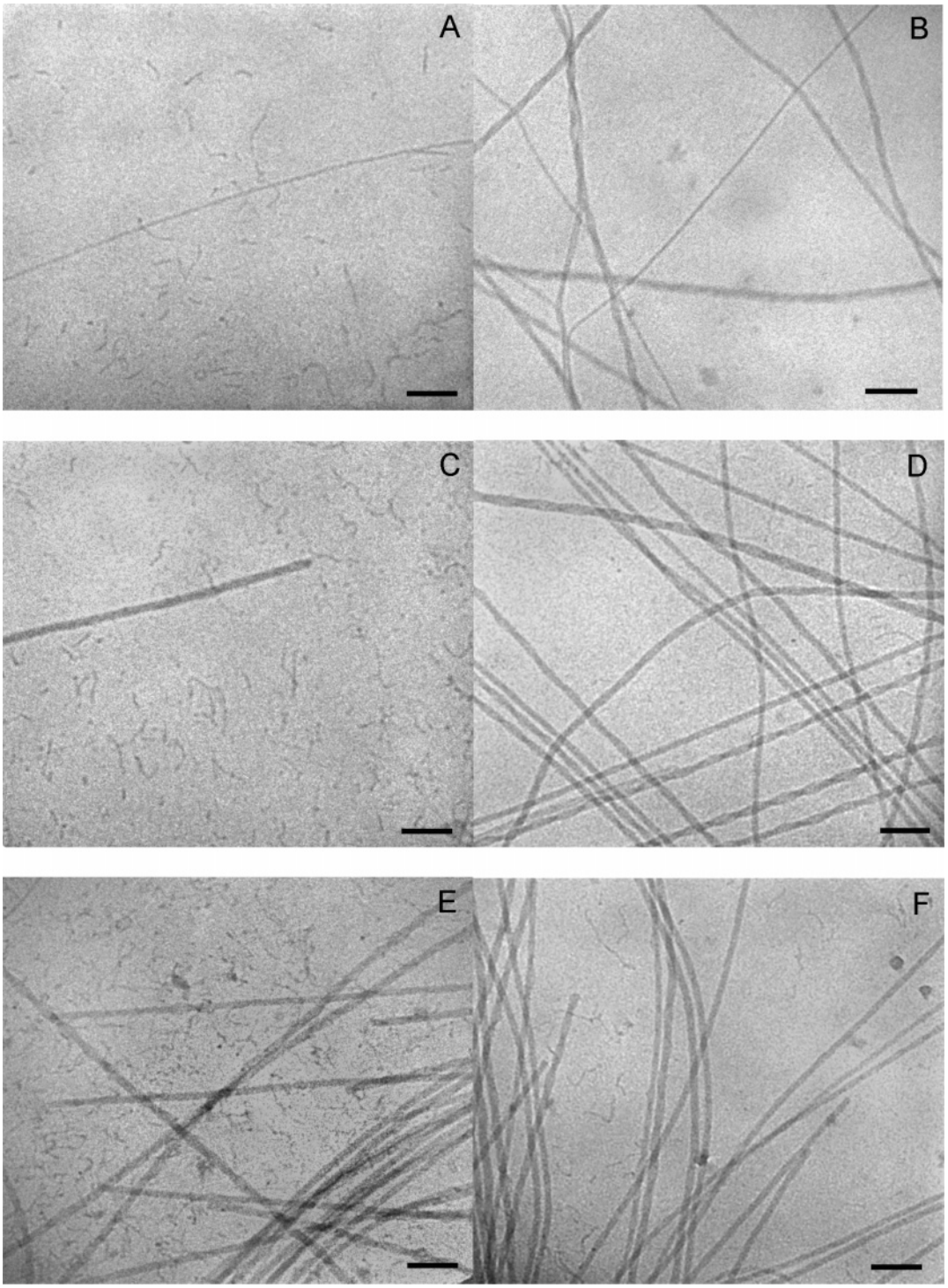

Figure 10. Cryo-TEM images of DLPM micellar solutions in in 0.1 M PBS pH = 7.5. The pictures on the left-hand side represent the samples just after the preparation at 25 °C, while those on the right-hand side are the same samples annealed at 25 °C for 2 days. DLPM concentrations: (A and B) 1 mM; (C and D) 4 mM; (E and F) 10 mM.

conformation both in supramolecular aggregates and in monophosphate monomer due to the poor stacking of the uridine base. CD spectra of DLPA are instead strongly affected by surfactant concentration: They show a remarkable increase of the molar ellipticities, more emphasized for the positive band, and a different absorption from AMP for all DLPA concentrations investigated.

This trend is also confirmed by the corresponding polynucleotide behavior in aqueous solutions at room temperature. In fact, while poly(U) is as a random coiled polymer and its CD intensity is only twice that of the monomer, poly(A) shows a much more intense CD signal than the monomer, in agreement with a stronger non-degenerate base stacking interaction.[30] Hence, this variation from the monomer signal indicates strong stacking excess in self-assembled structures as already observed for di-C_8P-nucleoside spherical micelles in 0.1 M PBS (pH = 7.5).[10]

It's important to underline that changes in CD spectra reflect changes in local structure, even if a structural interpretation from CD spectra is not always straightforward. In our case a striking parallelism with the structural observations obtained from light scattering and cryo-TEM occurs: While DLPU shows no concentration dependence as expected by the previous results,

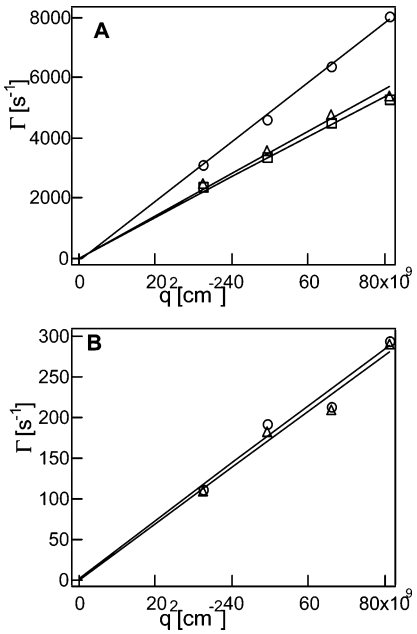

Figure 11. Relaxation modes of a 4 mM DLPM solution as a function of the scattering angle squared. (A) Behavior of Γ_1 (s^{-1}) (fast mode) vs q^2 (cm^{-2}): (○) just prepared; (□) annealed for 1 day; (△) annealed for 4 days. (B) Behavior of Γ_2 (s^{-1}) (slow mode) vs q^2 (cm^{-2}): (○) annealed for 1 day, (△) annealed for 4 days. The collective diffusion coefficients D_c (cm^{-2} s^{-1}) are obtained from the slopes of these fitting curves.

DLPA displays a consistently different behavior in the CD spectrum with the surfactant volume fraction.

The presence of a remarkable positive Cotton effect has been also observed for single-stranded poly(A), indicating a strong non-degenerate interaction (super-asymmetry involving the bases) related to base stacking. Particularly instructive for our purposes is the structural transition of poly(A) from the neutral pH form to the double-strand form (at acidic pH) qualitatively reflected in the CD spectrum by both a blue shift and an intensity increase. [31]

TABLE 2: Experimental Diffusion Coefficients for a 4 mM DLPM Micellar Solution Obtained from DLS Measurements

time	D_c fast (cm^2/s)	D_c slow (cm^2/s)
just prepared	$9.9 \times 10^{-8} \pm 2\%$	
after 1 day	$6.7 \times 10^{-8} \pm 2\%$	$3.5 \times 10^{-9} \pm 7\%$
after 4 days	$6.8 \times 10^{-8} \pm 5\%$	$3.5 \times 10^{-9} \pm 6\%$

The noteworthy positive Cotton effect for the lowest DLPA volume fractions can be ascribed to more pronounced stacking in this regime where the smaller micelles contribute to the intermicellar formation of the larger aggregates. We believe that the adenine environment changes, as the bases are involved in the intermicellar coordination to form twisted aggregates, inducing an increase in the positive signal. Hence more concentrated samples, where two phases coexist and contribute to the signal, show a slighter Cotton effect than the dilute ones.

In Figures 9a−c, we reported CD spectra of freshly and annealed samples at different surfactant concentrations to detect how self-assembling evolution influences the electronic properties of the bases.

As a general feature, fresh and annealed circular dichroic spectra differ in the position of the positive and negative maximum (a red shift), in the appearance of a new absorption around 206 nm, and in the decrease of the negative signal around 220 nm, irrespectively of surfactant concentration. We could not really relate these variations of CD signal to specific effects of base conformation or in supramolecular array, but they

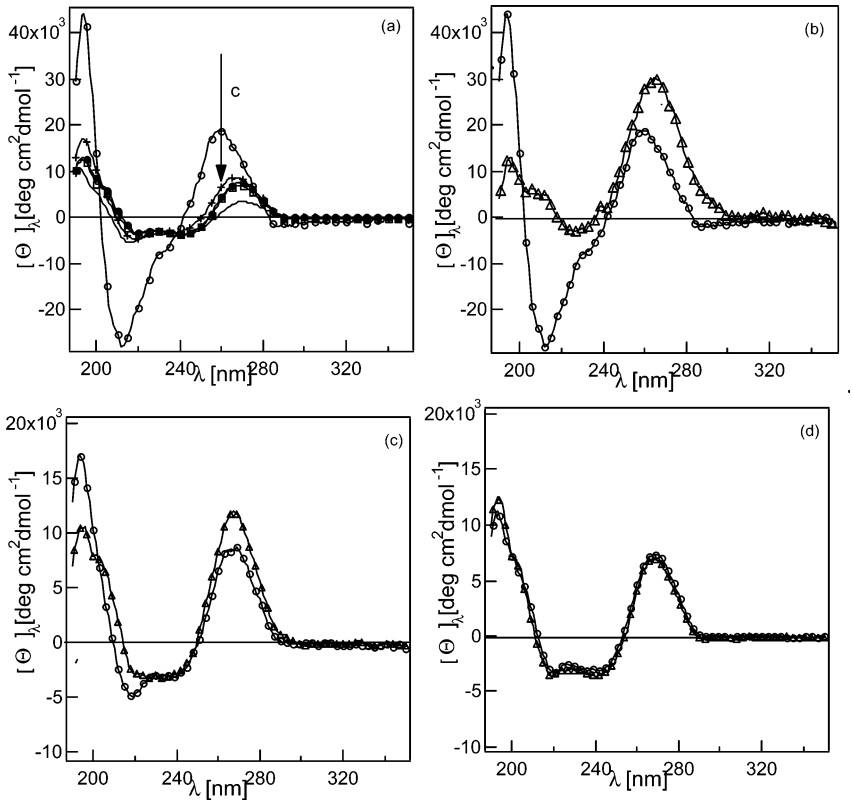

Figure 12. (a) Concentration dependence of CD spectra of DLPM micellar solutions in 0.1 M PBS pH = 7.5. Corresponding nucleosidic monophosphate monomer spectra (solid line), UMP + AMP (10 mM), are reported in the same medium, as well. The arrow indicates increasing DLPM concentrations. Surfactant concentrations: (○) 1 mM; (+) 4 mM; (●) 10 mM; (□) 20 mM. (b−d) CD spectra of DLPM micellar solutions in 0.1 M PBS at pH = 7.5 as a function of the time: (○) after 1 day; (△) after 3 days. (b) 1×10^{-3}M; (c) 4×10^{-3}M; (d) 1×10^{-2}M.

highlight that the structural evolution affects the base environment; i.e., base−base interactions have a meaningful role in DLPA self-assembling behavior.

DLP Mixture Self-Assembling Behavior. We have also investigated self-aggregation behavior of 1:1 mixture solutions of the two nucleolipids as a function of surfactant concentration to probe possible intramicellar interactions between complementary bases and how recogniton affects self-assembling.

Figures 10A−F report cryo-TEM images of DLPM micellar solutions, at the same surfactant concentration measured for DLPA, either just after lipid dissolution (left panel) or after 2 days annealing at 25 °C (right panel). The DLPM system behaves as DLPA and evolves to form giant superstructures for all the lipid concentrations investigated. The DLPA lipid seems to drive the self-assembling behavior even if some differences with respect to the pure component system can be detected: The helical twisting occurs at a lower percentage than in the corresponding DLPA samples, and giant aggregates are on average characterized by a smaller thickness. These effects can be attributed both to the decrease in base stacking caused by the pyrimidine doping and to the occurrence of hydrogen bonding selective interactions between the Watson−Crick complementary bases, as already observed for the short-chain micellar system.[10]

Finally, the introduction of the complementary nucleolipid locally affects the base environment inducing a different intra- and intermicellar coordination at the interface with respect to both pure nucleolipid systems that results in a behavior similar to that of DLPA but characterized by less tendency to form twisted aggregates. This confirms that the stacking interaction between purine bases is the predominant driving force for the twisting process.

To follow the evolution process of DLPM self-assembling aggregates, the mixture also has been nvestigated by dynamic light scattering experiments as a function of the annealing time. DLS experiments have been performed at different scattering angles to infer the nature of the resulting relaxation modes, choosing 4 mM as the total surfactant concentration.

The resulting intensity autocorrelation functions are monomodal right after sample preparation, while a second slower relaxation appears after 1 day and after 4 days for annealed samples. The mean relaxation rates Γ (s^{-1}) for both the fast and the slow modes have been obtained from the Laplace inversion of the autocorrelation functions using the CONTIN algorithm. The relaxation decay dependence from the squared scattering vector for both fast and slow modes is shown in Figures 11A and 11B; the resulting linear trend suggests a diffusive relaxation mechanism. Furthermore, the self-assembling process to form larger aggregates seems to occur predominantly in the first 24 h; in fact after 4 days both fast and slow relaxation times have not been significantly changed. In Table 2 we report the resulting collective diffusion coefficients, and they are of the same order of magnitude as the DLPA ones, only differing for the fast mode trend. The DLPA fast mode continues to increase a little bit even after first day while the DLPM fast mode remains constant. This behavior also indicates a lower tendency of the mixed lipid structures to aggregate, as already pointed out from cryo-TEM images.

CD experiments with DLPM micellar solutions as a function of lipid concentration (Figure 12a) confirm that mixed micelles essentially behave as DLPA solutions with a strong dependence of the CD signal on surfactant volume fractions. In particular, they show an increase of the molar ellipticities, more emphasized for lower surfactant concentrations, with respect to the mono-

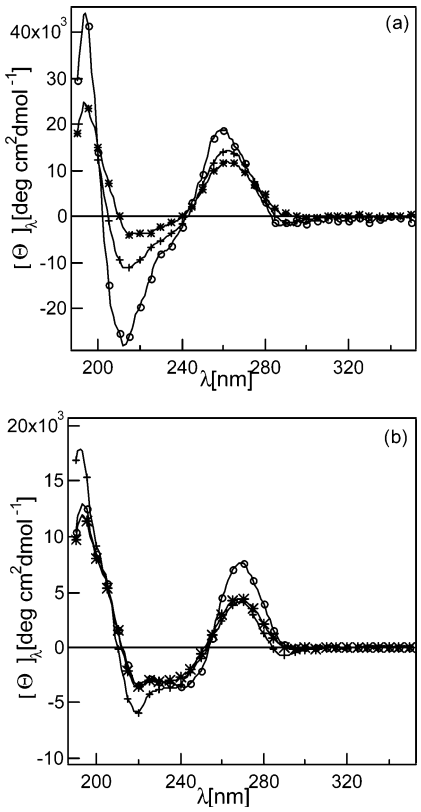

Figure 13. CD spectra of DLPM micellar solutions compared to the average spectrum of the pure components (each at the same total lipid concentration as in DLPM sample) and to the sum of the spectra of the pure dlpn components (each at the half lipid concentration of the total one in DLPM sample): (○) DLPM; (∗) average spectrum; (+) sum spectrum. (a) DLPM concentration is 1×10^{-3} M. (b) DLPM concentration is 2×10^{-2} M.

nucleotide spectra. This effect is more remarkable for the positive band than for the negative one where spectra are very similar.

An exception is found for the most dilute sample that displays a larger effect for the negative band. DLPM CD spectra of the more concentrated samples are similar to the monomer mixture signal, indicating that the super-asymmetry of the aggregate decreases as the concentration is increased, eventually reaching a concentration-invariant regime. Furthermore, a CD study as a function of the annealing time (Figures 12b−d) has pointed out that the more remarkable effects occur at lower surfactant concentrations; dlpm spectra do not show any change for surfactant concentrations higher than 1×10^{-2} M.

It is also important to consider whether the 1:1 mixture of the two lipids shows deviation from what is expected in the case of ideal mixing to deduce the possible presence of specific interactions between nucleic bases at the interface. In fact, a nonideal behavior indicates preferential interactions between a purinic base and a pyrimidinic base that is molecular recognition in a Watson−Crick context. The comparison, in this case, is complicated by the concentration dependence of DLPA dichroism that has to be taken into account. Figures 13a and 13b show, respectively, for total lipid concentrations of 1×10^{-3} and 2×10^{-2} mol/L, the spectrum of the mixture compared to the average spectra obtained from the 1×10^{-3} and 2×10^{-2} mol/L pure lipids and the sum of the spectra obtained for the 5×10^{-4} and 1×10^{-2} mol/L pure lipids.

The deviation either from the ideal mixing or from the segregation of the lipids is straightforward, indicating stacking excess for both the samples.

Conclusions

Dilauroyl-phosphatidyl-adenosine, dilauroyl-phosphatidyl-uridine, and their 1:1 mixture self-assemble in solution forming, in the experimental conditions used in this study, wormlike micelles. The adenosine derivative and the mixture, formed from the two complementary adenosine and uridine nucleolipids, evolve during aging into helicoidal suprastructures that are formed at the expense of the wormlike micelles. Evidence for this process was obtained by the combined analysis of dynamic light scattering and cryo-TEM investigations. The lipids investigated differ from each other only for the nucleoside that constitutes the lipid polar head suggesting that the different structures formed in solution are a consequence of the different stacking (purine−purine > purine−pyrimidine > pyrimidine−pyrimidine) and hydrogen bonding capacities of the adenosine and uridine bases. Circular dichroism confirms that the stacking interaction between purine bases is the driving force in the helix formation.

Acknowledgment. Thanks are due to professor Barry Ninham for helpful discussions, to Consorzio Interuniveristario per lo Sviluppo dei Sistemi a Grande Interfase), and to the European Union (Grant No. NMP4-CT-2004-013575 AMNA-STREEP) for financial support.

References and Notes

(1) Baglioni, P.; Berti, D. *Curr. Opin. Colloid Interface Sci.* **2003**, *8*, 55.
(2) Mirkin, C. A. *Inorg. Chem.* **2000**, *39*, 2258.
(3) Mirkin, C. A.; Letsinger, R. L.; Mucic, R. C.; Storhoff, J. J. *Nature* **1996**, *382*, 607.
(4) Niemeyer, C. M. *Angew. Chem., Int. Ed.* **2001**, *40*, 4128.
(5) Niemeyer, C. M. *Trends Biotechnol.* **2002**, *20*, 395.
(6) Berti, D.; Keiderling, U.; Baglioni, P. *Prog. Colloid Polym. Sci.* **2002**, *120*, 64.
(7) Berti, D. Franchi, L.; Baglioni, P.; Luisi, P. L. *Langmuir* **1997**, *13*, 3438.
(8) Berti, D.; Luisi, P. L.; Baglioni, P. *Colloids Surf., A* **2000**, *167*, 95.
(9) Berti, D., Pini, F.; Teixeira, J.; Baglioni, P. *J. Phys. Chem. B* **1999**, *103*, 1738.
(10) Berti, D.; Barbaro, P. L.; Bucci, I.; Baglioni, P. *J. Phys. Chem B* **1999**, *103*, 4916.
(11) Berti, D.; Baldelli Bombelli, F.; Almgren, M.; Baglioni, P. In *Self-Assembly*; Robinson, B., Ed.; IOS Press: Amsterdam, 2003.
(12) Baldelli Bombelli, F.; Berti, D.; Keiderling, U.; Baglioni, P. *J. Phys. Chem. B* **2002**, *106*, 11613.
(13) Baldelli Bombelli, F.; Berti, D.; Keiderling, U.; Baglioni, P. *Appl. Phys. A: Mater. Sci. Process.* **2002**, *74* (Suppl.), S1270.
(14) Shuto, S. U., S.; Imamura, S.; Fukukawa, K.; Tsujino, M.; Matsuda, A.; Ueda, T. *Chem. Pharm. Bull.* **1988**, *36*, 209.
(15) Provencher, S. W. *Comput. Phys. Commun.* **1982**, *27*, 213.
(16) Mays, H. A., M.; Dedinaite, A.; Claesson, P. M. *Langmuir* **1999**, *23*, 8072−8079.
(17) Baldelli Bombelli, F.; Berti, D.; Pini, F.; Keiderling, U.; Baglioni, P. *J. Phys. Chem. B* **2004**, *108*, 16427.
(18) Shimizu, T.; Hato, M. *Biochim. Biophys. Acta* **1993**, *1216*, 126.
(19) Lowik, D. W. P. M.; Garcia-Hartjes, J.; Meijer, J. T.; van Hest, J. C. M. *Langmuir*, **2005**, *21*, 524.
(20) Schnur, J. M. *Science* **1993**, *262*, 1669.
(21) Yanagawa, H.; Ogawa, Y.; Furuta, H.; Tsuno, K. *J. Am. Chem. Soc.* **1989**, *111*, 4567.
(22) Oda, R.; Huc, I.; Schmutz, M.; Candau, S. J.; Mackintosh, F. C. *Nature* **1999**, *399*, 566.
(23) Selinger, J. V.; Spector, M. S.; Schnur, J. M. *J. Phys. Chem. B* **2001**, *105*, 7157.
(24) Goodby, J. W. *J. Mater. Chem.* **1991**, *1*, 307.
(25) Haasnoot, C. A. G.; Altona, C. *Nucleic Acids Res.* **1979**, *6*, 1135.
(26) Saenger, W. *Angew. Chem., Int. Ed. Engl.* **1973**, *12*, 591.
(27) Saenger, W. *Angew. Chem.* **1973**, *85*, 680.
(28) Curtis Johnson, W. CD of Nucleic Acid. In *Circular Dichroism: Principles and Application*; Nakanishi, K., Berova, N., Woody, R. J., Ed.; Wiley-VCH: New York., 1994; Chapter 19; p 523.
(29) Curtis Johnson, W. CD and Its Empirical Application to Biopolymers. In *Methods of Biochemicals Analysis*; Wiley: New York, 1985; Vol. 31; p 61.
(30) Brahms, J.; Maurizot, J. C.; Michelson, A. M. *J. Mol. Biol.* **1967**, *25*, 481.
(31) Brahms, J.; Michelson, A. M.; Van Holde, K. E. *J. Mol. Biol.* **1966**, *15*, 467.